Interleukin-8 dysregulation is implicated in brain dysmaturation following preterm birth.

Brain, Behavior, and Immunity xxx (xxxx) xxx–xxx

Contents lists available at ScienceDirect

Brain, Behavior, and Immunity

journal homepage: www.elsevier.com/locate/ybrbi

Interleukin-8 dysregulation is implicated in brain dysmaturation following preterm birth

Gemma Sullivan[a], Paola Galdi[a], Manuel Blesa Cabez[a], Nis Borbye-Lorenzen[b], David Q. Stoye[a], Gillian J. Lamb[a], Margaret J. Evans[c], Alan J. Quigley[d], Michael J. Thrippleton[e,f], Kristin Skogstrand[b], Siddharthan Chandran[e,g], Mark E. Bastin[e], James P. Boardman[a,e,*]

[a] MRC Centre for Reproductive Health, University of Edinburgh, Edinburgh, UK
[b] Danish Center for Neonatal Screening, Department of Congenital Disorders, Statens Serum Institut, Copenhagen, Denmark
[c] Department of Pathology, Royal Infirmary of Edinburgh, Edinburgh, UK
[d] Department of Radiology, Royal Hospital for Sick Children, Edinburgh, UK
[e] Centre for Clinical Brain Sciences, University of Edinburgh, Edinburgh, UK
[f] Edinburgh Imaging, University of Edinburgh, Edinburgh, UK
[g] MRC Centre for Regenerative Medicine, University of Edinburgh, UK

ARTICLE INFO

Keywords:
Preterm
Neonate
Inflammation
Interleukin-8
Magnetic resonance imaging
Brain

ABSTRACT

Background: Preterm birth is associated with dysconnectivity of structural brain networks, impaired cognition and psychiatric disease. Systemic inflammation contributes to cerebral dysconnectivity, but the immune mediators driving this association are poorly understood. We analysed information from placenta, umbilical cord and neonatal blood, and brain MRI to determine which immune mediators link perinatal systemic inflammation with dysconnectivity of structural brain networks.

Methods: Participants were 102 preterm infants (mean gestational age 29^{+1} weeks, range 23^{+3}-32^{+0}). Placental histopathology identified reaction patterns indicative of histologic chorioamnionitis (HCA), and a customized immunoassay of 24 inflammation-associated proteins selected to reflect the neonatal innate and adaptive immune response was performed from umbilical cord (n = 55) and postnatal day 5 blood samples (n = 71). Brain MRI scans were acquired at term-equivalent age (41^{+0} weeks [range 38^{+0}-44^{+4} weeks]) and alterations in white matter connectivity were inferred from mean diffusivity and neurite density index across the white matter skeleton.

Results: HCA was associated with elevated concentrations of C5a, C9, CRP, IL-1β, IL-6, IL-8 and MCP-1 in cord blood, and IL-8 concentration predicted HCA with an area under the receiver operator curve of 0.917 (95% CI 0.841 – 0.993, $p < 0.001$). Fourteen analytes explained 66% of the variance in the postnatal profile (BDNF, C3, C5a, C9, CRP, IL-1β, IL-6, IL-8, IL-18, MCP-1, MIP-1β, MMP-9, RANTES and TNF-α). Of these, IL-8 was associated with altered neurite density index across the white matter skeleton after adjustment for gestational age at birth and at scan ($\beta = 0.221$, $p = 0.037$).

Conclusions: These findings suggest that IL-8 dysregulation has a role in linking perinatal systemic inflammation and atypical white matter development in preterm infants.

1. Introduction

Preterm birth affects around 15 million births annually (Chawanpaiboon et al., 2019), and is an important cause of cerebral palsy, cognitive impairment, autism spectrum disorder and psychiatric disease later in life (Twilhaar et al., 2018). Magnetic resonance imaging (MRI) studies reveal a cerebral phenotype of preterm birth that is associated with later function, and includes diffuse white matter disease, dysconnectivity of developing networks, and structural alterations in cortical and deep grey matter (Ball et al., 2017; Batalle et al., 2017; Boardman et al., 2010; Galdi et al., 2020; Kapellou et al., 2006). These image features are manifest by term-equivalent age, which suggests that interventions to prevent injury and restore typical development may need to be applied during the perinatal period.

Immune dysregulation at a critical point in neurodevelopment is strongly implicated in the pathogenesis of the encephalopathy of

* Corresponding author at: MRC Centre for Reproductive Health, University of Edinburgh, Edinburgh, UK.
E-mail address: james.boardman@ed.ac.uk (J.P. Boardman).

https://doi.org/10.1016/j.bbi.2020.09.007
Received 20 May 2020; Received in revised form 5 September 2020; Accepted 5 September 2020

prematurity, which can be conceptualized as white matter injury and subsequent dysmaturation of diverse cellular processes resulting in atypical development of white and grey matter structures (Hagberg et al., 2015; Volpe, 2019). Preterm infants have a distinct inflammatory profile in blood and cerebrospinal fluid (CSF) that includes higher levels of pro-inflammatory cytokines and lower levels of neuroprotective growth factors compared to infants born at term (Boardman et al., 2018; Skogstrand et al., 2008), and there is evidence that both systemic inflammation and neuroinflammation are associated with overt forms of preterm brain injury. For example, elevated IL-1β, IL-6, IL-8 and IL-10 in umbilical cord and early postnatal blood is associated with intraventricular hemorrhage and white matter lesions soon after birth (Duggan et al., 2001; Leviton et al., 2018; Yoon et al., 1996), and persistently elevated pro-inflammatory proteins during the first 2 weeks after preterm birth are associated with increased risk of cerebral palsy (Carlo et al., 2011; Kuban et al., 2014) and impaired neurocognitive development in infancy and childhood (Hansen-Pupp et al., 2008; Kuban et al., 2017; Leviton et al., 2016; O'Shea et al., 2012, 2013; Yanni et al., 2017). Furthermore, specific co-morbidities of preterm birth characterized by systemic inflammation, including intrauterine inflammation (histologic chorioamnionitis, HCA) and necrotizing enterocolitis, are associated with abnormal white matter on magnetic resonance imaging (Anblagan et al., 2016; Ball et al., 2017; Barnett et al., 2018; Shah et al., 2008). However, previous study designs leave uncertainty about which immune mediators are associated with white matter dysmaturation and network dysconnectivity.

Diffusion tensor MRI (DTI) and neurite orientation dispersion and density imaging (NODDI) support inference about the microstructural properties of developing white matter (Pietsch et al., 2019; Tariq et al., 2016; Zhang et al., 2012). Specifically, normal brain maturation is characterized by a reduction in white matter mean diffusivity (MD) and an increase in neurite density index (NDI); but MD is increased and NDI decreased in preterm infants at term equivalent age, compared with healthy controls infants born at term (Pecheva et al., 2018). These changes reflect an increase in water content and a decrease in white matter organization in preterm infants. Peak width of skeletonised mean diffusivity (PSMD) is a method for histogram based calculation of MD distribution across the entire white matter skeleton, which provides a measure of generalized white matter microstructure and dysconnectivity that is related to cognition (Baykara et al., 2016; Deary et al., 2019; Wei et al., 2019). In previous work we extended the histogram model to include peak width of skeletonised neurite density index (PSNDI) and found that PSMD and PSNDI are both altered in preterm infants at term equivalent age, indicating that these are useful biomarkers of generalized white matter connectivity in the developing brain (Blesa et al., 2020).

Identification of immune mediators of generalized dysconnectivity during the perinatal period is important for elucidating new targets for neuroprotection therapies. In this study, we utilized an immunoassay of 24 analytes customized to reflect perinatal innate and adaptive immune responses, and analyzed profiles from umbilical cord and postnatal blood samples with placental histopathology and brain MRI to test the hypothesis that specific immune mediators link systemic inflammation with atypical white matter development in preterm infants. We found that elevated IL-8 is a characteristic feature of intrauterine and postnatal systemic inflammation, and it is associated with white matter dysconnectivity in preterm infants.

2. Methods and materials

2.1. Participants

Participants were 102 preterm infants born $\leq 32^{+0}$ weeks' gestation, delivered at the Royal Infirmary of Edinburgh, UK and recruited to a longitudinal study of the effect of preterm birth on brain development and long term outcome (Boardman et al., 2020). Exclusion criteria included infants with major congenital abnormality, post-hemorrhagic ventricular dilatation, cystic periventricular leukomalacia, or contraindications to MRI. Ethical approval was obtained from the UK National Research Ethics Service and parents provided written informed consent (South East Scotland Research Ethics Committee 16/SS/0154). Subsets were used to investigate relationships between inflammatory mediators in umbilical cord blood and HCA (n = 55), and between inflammation in the postnatal period and MRI markers of white matter connectivity (n = 71).

2.2. Blood sample collection

2.2.1. Collection procedure

Dried blood spot samples (DBSS) were taken from the umbilical cord following delivery and from blood drawn on day 5 of life using a FTA™ DMPK-A Card (Whatman™ GE Healthcare). Bloodspot cards were dried at room temperature and then stored at −20 °C until analysis at the Statens Serum Institut (Center for Neonatal Screening, Copenhagen, Denmark). A customized multiple sandwich immunoassay based on meso-scale technology was used to measure blood spot levels of Interleukin (IL)1-β, IL-2, IL-4, IL-5, IL-6, IL-8, IL-10, IL-12p70, IL-17, IL-18, Monocyte chemotactic protein-1 (MCP-1), Macrophage inflammatory protein-1α (MIP-1α), Macrophage inflammatory protein-1β (MIP-1β), Tumor necrosis factor-α (TNF-α), Tumor necrosis factor-β (TNF-β), Brain-derived neurotrophic factor (BDNF), Granulocyte-macrophage colony-stimulating factor (GM-CSF), Interferon-γ (IFN-γ), C-reactive protein (CRP), matrix-metalloproteinase 9 (MMP-9), Regulated upon activation, normal T cell expressed and secreted (RANTES) and Complement components C3, C5a and C9.

2.2.2. Dried blood spot sample analysis

Two 3.2 mm disks from the DBSS were punched into each well of Nunc 96-well polystyrene microwell plates (#277143, Thermo Fisher Scientific). 130 μl extraction buffer (PBS containing 1% BSA (Sigma Aldrich #A4503), 0.5% Tween-20 (#8.22184.0500, Merck Millipore), and complete protease inhibitor cocktail (#11836145001, Roche Diagnostics)) was added to each well, and the samples were incubated for 1 h at room temperature on a microwell shaker set at (900 rpm). The extracts were analyzed using U-plex plates (Meso-Scale Diagnostics (MSD), Maryland, US) coated with antibodies specific for IL-1β, IL-2, IL-4, IL-5, IL-6, IL-8, IL-12, IL-17, TNF-α, MIP-1β on one plate (#K15067 customized) and BDNF, GM-CSF, IL-10, IL-18, IFN-γ, TNF-β, MCP-1, MIP-1α on another (#K151AC customized) (both MSD). Supplier's instructions were followed, and extracts were analysed undiluted. A third multiplex analysis was developed in-house applying extracts diluted 1:10 in diluent 7 (#R54BB, MSD) using antibodies specific for C3 (HYB030-07 and HYB030-06, SSI Antibodies, Copenhagen, Denmark), C5a (10604-MM04 and 10604-MM06, Sino Biological, Eschborn, Germany), C9 (R-plex kit #F21XZ, MSD), MMP-9 (BAF911 and MAB911), RANTES (MAB278 and AF278NA) and CRP (BAM17072 and MAB1701) (all R&D Systems, Minneapolis, US) for coating the U-plex plate and for detection, respectively. Coating antibodies (used at 1 μg/mL, except CRP used at 10 ng/mL) were biotinylated (using EZ-Link Sulfo-NHS-LC-Biotin #21327, Thermo Fisher Scientific) in-house (if not already biotinylated at purchase) and detection antibodies were SULFO-tagged (R91AO, MSD), both at a challenge ratio of 20:1. The following calibrators were used: C3: #PSP-109 (Nordic Biosite, Copenhagen, DK), C5a: #10604-HNAE (Sino Biological), C9: #F21XZ (from R-plex kit, MSD), MMP-9: #911-MP, RANTES: #278-RN and CRP: #1707-CR/CF (all from R&D Systems). Calibrators were diluted in diluent 7, detection antibodies (used at 1 μg/mL, except CRP used at 100 ng/mL) were diluted in diluent 3 (#R50AP, MSD). Controls were made in-house from part of the calibrator solution in one batch, aliquoted in portions for each plate and stored at −20 °C until use. The samples were prepared on the plates as recommended from the manufacturer and were immediately read on the QuickPlex SQ 120 (MSD).

Analyte concentrations were calculated from the calibrator curves on each plate using 4PL logistic regression using the MSD Workbench software.

2.2.3. Analytical characterization

Intra-assay variations were calculated from 16 measurements of a pool of the same control sample on the same plate. Inter-assay variations were calculated from controls analyzed in duplicate on each plate during the sample analysis, 4 plates in total. Limit of detections were calculated as 2.5 standard deviations from duplicate measurements of the zero calibrator. The higher detection limit was defined as the highest calibrator concentration. The median intra-assay variation was 8.2% and median inter-assay variation was 11.1%. The inter-assay variation was largely influenced by CRP, RANTES and MMP-9. Detection limits and assay variations are shown in Supplementary Table S1.

2.3. Placental histopathology

Placental examination was performed by an experienced perinatal pathologist (M.J.E.) and placental reaction patterns were reported according to the site and degree of inflammation, using a structured system (Redline et al., 2003). HCA was defined as the presence of an inflammatory response in the placental membranes of any grade or stage.

2.4. Magnetic resonance imaging

2.4.1. MRI procedure

Structural and diffusion MRI brain scans were performed at mean gestational age (GA) 41^{+0} weeks (range 38^{+0}-44^{+4} weeks). Infants were scanned in natural sleep with monitoring of pulse oximetry, electrocardiography and temperature. For ear protection, flexible earplugs and neonatal earmuffs (MiniMuffs, Natus Medical Inc., CA) were used. All scans were supervised by a neonatal doctor and research midwife. MRI scans were performed on a Siemens Magnetom Verio 3T scanner (Siemens Healthcare, Erlangen, Germany) using a 16-channel phased array head coil. Infants were scanned to acquire: 3D T1-weighted (T1w) MPRAGE volume (TR = 1970 ms, TE = 4.69 ms, inversion time = 1100 ms, flip angle = 9° acquisition plane = sagittal, voxel size = 1 × 1 × 1 mm^3, FOV = 160 mm, acquisition time = 3:09), axial T2-weighted BLADE (TR = 4100 ms, TE = 207 ms, voxel size = 0.7 × 0.7 × 3.0 mm^3, FOV = 220 mm, acquisition time = 2:29), T2-weighted SPACE (TR = 3200 ms, TE = 409 ms, acquisition plane = sagittal, voxel size 1 × 1 × 1 mm^3, FOV = 128 mm, acquisition time = 2:13), SWI (TR = 28 ms, TE = 20 ms, voxel size = 0.8 × 0.8 × 3.0 mm^3, acquisition time = 2:23) and axial T2-weighted FLAIR BLADE (TR = 10000, TE = 130, voxel size = 0.9 × 0.9 × 3.0 mm^3, acquisition time = 3:22). Diffusion MRI data were acquired in 2 parts with interspersed T2-weighted (b = 0 s/mm^2) volumes: part 1 consisting of 8b = 0 s/mm^2 and 64 diffusion-weighted b = 750 s/mm^2, and part 2 consisting of 8b = 0 s/mm^2, 3b = 200 s/mm^2, 6b = 500 s/mm^2 and 64b = 2500 s/mm^2 single-shot spin-echo echo planar imaging (EPI) volumes acquired with 2 mm isotropic voxels (TR = 3500 ms, TE = 78 ms, FOV = 256 mm, acquired matrix 128 × 128, acquisition time 4:29 + 5:01) (Boardman et al., 2020).

Structural images were reported by a pediatric radiologist with experience in neonatal MRI (A.J.Q.) using an established system (Leuchter et al., 2014). Images with evidence of post-hemorrhagic ventricular dilatation, cystic periventricular leukomalacia or central nervous system malformation were excluded.

2.4.2. MRI analysis

Diffusion MRI volumes were denoised using a Marchenko-Pastur-PCA based algorithm (Tournier et al., 2019; Veraart et al., 2016). Eddy current, head movement and EPI geometric distortions were corrected using outlier replacement and slice-to-volume registration (Andersson et al., 2003, 2017, 2016; Andersson and Sotiropoulos, 2016; Jenkinson et al., 2012) and bias field inhomogeneity correction was applied (Tustison et al., 2010). A template was constructed using data from 50 term born infants using DTI-TK and all the subjects were aligned (Blesa et al., 2020; Zhang et al., 2006). The water diffusion tensor derived maps of each subject were calculated after registration. The NODDI maps were calculated in the subject's native space with the NODDI-Bingham model using cuDIMOT (Hernandez-Fernandez et al., 2019; Tariq et al., 2016) and then the intracellular volume fraction [NDI] was propagated to the template space using the previously calculated transformations. The main skeleton of the fractional anisotropy (FA) template was created by thresholding at 0.15, and individual FA maps were projected onto this skeleton. Using this projection, the remaining maps were also projected to the white matter skeleton. A custom mask was created by editing the skeleton mask to remove CSF and grey matter contaminated areas, and by removing tracts passing through the cerebellum, the brainstem and subcortical grey matter areas. The resulting skeletonized maps were then multiplied by the custom mask. PSMD and PSNDI were calculated as the difference between the 95th and 5th percentiles on histogram analysis (Blesa et al., 2020). Fig. 1 summarizes the pipeline for calculation of histogram based metrics.

2.5. Statistical analysis

Participant characteristics were compared using Student's *t*-test or Mann-Whitney U to compare distributions, and Chi-square tests were used to compare proportions. To investigate group differences in immune mediator profiles between those with and without HCA we used the Mann-Whitney U test and Bonferroni correction for multiple tests. Associations that remained significant after Bonferroni correction were analysed in logistic regression models where HCA was the dependent variable, analyte concentration was the independent variable, and GA at birth was entered as a covariate. The predictive power of those analytes that were associated with HCA after adjustment for GA at birth was determined using receiver operator characteristic (ROC) analysis.

To investigate relationships between systemic inflammation and white matter microstructure, principal component analysis (PCA) was used to identify blood analytes contributing to variance in the postnatal inflammatory profile. Analytes that contributed to PCs with eigenvalues > 1 were entered as independent variables in multivariable linear regression models with PSMD and PSNDI as dependent variables, and GA at birth and scan as covariates.

For all analyses, analytes with values less than the lower limit of detection (< LOD) were assigned the lowest detectable level prior to statistical analysis, and analytes with concentrations < LOD in ≥75% of participants were excluded. Statistical analyses were performed using SPSS version 24.0 (IBM Corp., Armonk, NY), with the exception of PCA, which was performed using R version 3.6.1 (R Core Team, 2019).

3. Results

3.1. Participants

One hundred and two preterm infants (born before 32 weeks of gestation) took part, and their clinical characteristics are shown in Table 1. Fifty-five infants had umbilical cord blood obtained immediately following delivery, and seventy-one infants had blood taken on postnatal day 5 and had MRI performed at term-equivalent age.

3.2. Umbilical cord blood inflammatory profile associated with histologic chorioamnionitis

Of 55 infants with umbilical cord blood sampling and placental

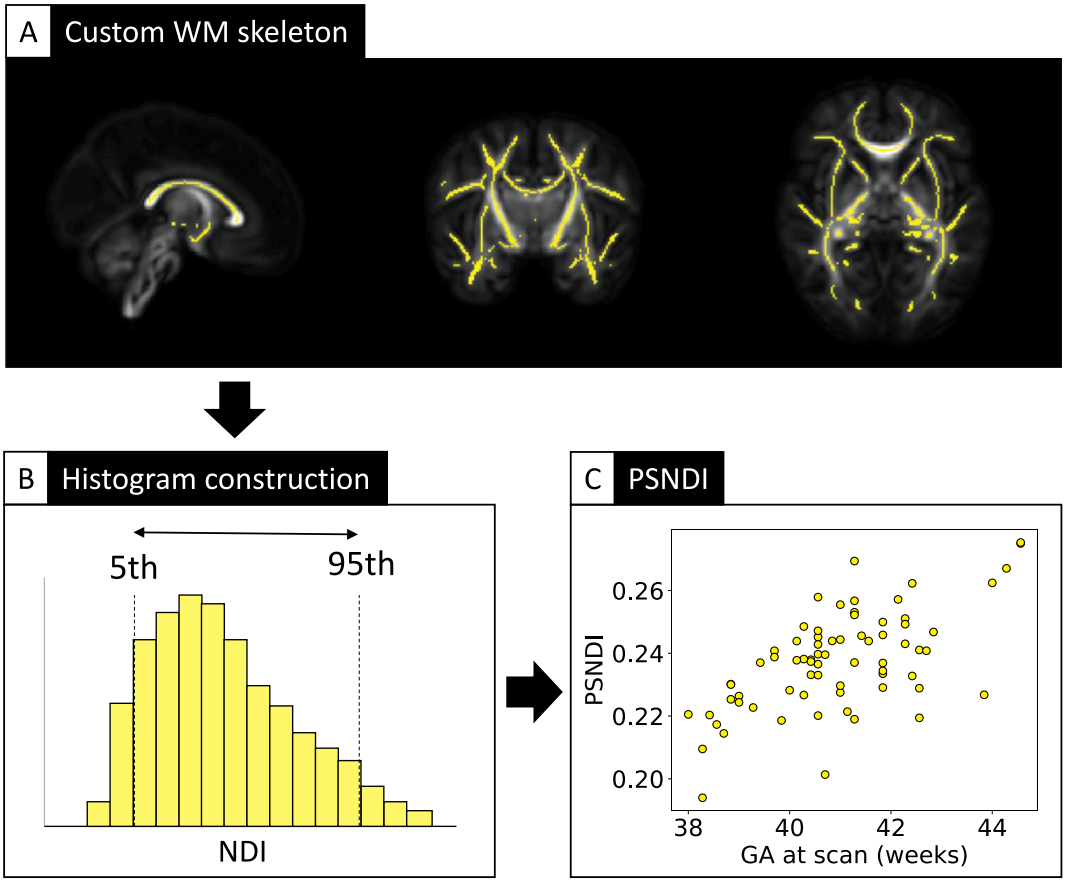

Fig. 1. Imaging pipeline for the construction of PSNDI. (A) shows the custom white matter skeleton, (B) shows the calculation of PSNDI from a histogram analysis of neurite density index, and (C) shows a scatterplot of PSNDI versus gestational age at MRI scan.

histopathology, 24 (44%) were exposed to HCA during fetal life. Infants with HCA exposure had lower GA at birth than infants without HCA: mean GA 28^{+0} weeks versus 29^{+5} weeks ($p = 0.002$). There were no statistically significant group differences in birthweight, infant sex, or exposures to antenatal corticosteroids or magnesium sulphate for fetal neuroprotection.

Ten of the 24 analytes had concentrations < LOD in ≥ 75% of both groups and were therefore excluded from subsequent analyses. Table 2 shows umbilical cord blood analyte concentrations for infants exposed to HCA and infants without HCA. Those exposed to HCA had higher cord blood levels of C5a, C9, CRP, IL-1β, IL-6, IL-8 and MCP-1 ($p < 0.003$, Bonferroni corrected). Of these 7 analytes, 5 were associated with HCA after adjustment for GA at birth in regression models: C5a, IL-1β, IL-6, IL-8 and MCP-1 (β between 0.88 and 28.78, $p < 0.05$). IL-8 concentration was the best predictor of HCA with an area under the curve (AUC) of 0.917 (SE 0.039), 95% CI 0.841 – 0.993, $p < 0.001$ (Fig. 2, Supplementary Table S2).

3.3. Postnatal inflammation and white matter microstructure

We investigated whether specific components of the perinatal immune profile are associated with white matter microstructure (PSNDI and PSMD), by studying a subset of infants who had their inflammatory profile sampled on postnatal day 5 and brain MRI at term-equivalent

Table 1
Clinical characteristics of participants.

Sample subset	HCA prediction n = 55	MRI brain n = 71
Mean GA at birth, weeks (range)	29^{+0} (23^{+3}-32^{+0})	29^{+4} (23^{+6}-32^{+0})
Proportion of male infants (%)	60	58
Antenatal steroids, any (%)	98	96
Antenatal magnesium sulphate, any (%)	95	93
Mean birthweight, g (range)	1202 (454–2110)	1284 (600–2060)
Histologic chorioamnionitis, HCA (%)	44	30
Sepsis (%)	–	18
Necrotizing enterocolitis, NEC (%)	–	6
Bronchopulmonary dysplasia, BPD (%)	–	25
Retinopathy of prematurity, ROP (%)	–	6
Mean GA at scan, weeks (range)	–	41^{+0} (38^{+0}-44^{+4})

Sepsis: Positive blood culture with a pathogenic organism, or blood culture positive for coagulase negative staphylococcus / negative and treatment course for ≥5 days. Necrotizing enterocolitis: medical treatment for ≥7 days or surgical treatment. Bronchopulmonary dysplasia: the need for supplemental oxygen therapy or respiratory support at 36^{+0} weeks gestational age. Retinopathy of prematurity: requiring treatment with laser therapy.

Table 2
Concentrations of analytes measured from dried blood spots taken from umbilical cord blood of preterm infants with and without exposure to histologic chorioamnionitis.

	No HCA (n = 31)		HCA (n = 24)		
Analyte (pg/ml)	Median	Q1-Q3	Median	Q1-Q3	p value
BDNF	21.4	4.1–30.8	29.3	6.2–48.2	0.072
C3	2451737.0	1655563.9–3373401.2	3859628.4	2265098.7–6336222.3	0.03
C5a	2779.7	1943.1–4172.1	6202.1	3611.9–16932.6	< 0.001
C9	583.0	153.7–1483.2	4857.0	1285.0–38747.0	< 0.001
CRP	89.0	89.0–195.0	8829.8	89.0–100702.7	0.001
IL-1β	0.0	0.0–0.0	0.5	0.0–0.9	< 0.001
IL-6	0.5	0.5–0.5	5.201	0.6–23.2	< 0.001
IL-8	7.5	3.4–12.1	106.7	25.5–496.4	< 0.001
IL-18	28.1	15.4–47.9	14.5	8.4–35.8	0.06
MCP-1	85.4	65.1–117.2	206.8	104.1–364.5	< 0.001
MIP-1β	8.9	4.3–16.8	16.1	11.1–29.9	0.04
MMP-9	11681.7	2139.0–20169.1	16664.4	5242.5–70313.8	0.127
RANTES	1311.4	617.6–2754.4	1540.7	715.6–3349.5	0.519
TNF-α	0.3	0.3–0.6	0.3	0.3–0.3	0.619

age.

The mean peak width of skeletonized neurite density index (PSNDI) for the group was 0.238 mm^2sec^{-1} $x10^{-3}$ (SD 0.016), and mean PSMD was 0.601 mm^2sec^{-1} $x10^{-3}$ (SD 0.062).

Using principal component analysis, we found that five PCs (eigenvalues > 1) explained 66% of the variance in the postnatal inflammatory profile, with most variance explained by the first two PCs (23% and 15% respectively), Supplementary Table S3. Fourteen analytes contributed to the 5 PCs: BDNF, C3, C5a, C9, CRP, IL-1β, IL-6, IL-8, IL-18, MCP-1, MIP-1β, MMP-9, RANTES and TNF-α (Supplementary Fig. S4).

Of these 14 analytes, IL-8 was the only one to be associated with PSNDI (β = 0.221, p = 0.037), in a multivariable model that explained 48% of the variance in PSNDI at term-equivalent age (F (16,54) = 5.09, R^2 adjusted = 0.48, p < 0.001) (Fig. 3, Supplementary Table S5). None of the remaining 13 analytes were associated with PSNDI and there were no significant associations between any analyte and PSMD.

4. Discussion

By combining data from placenta, blood and brain MRI we have shown that IL-8 dysregulation may link systemic inflammation during perinatal life with altered white matter development in preterm infants. We found that umbilical cord blood IL-8 concentration was strongly predictive of histologic chorioamnionitis, which is an intrauterine inflammatory condition and leading cause of preterm birth, and that elevated IL-8 in the first week of postnatal life is associated with white matter dysmaturation at term-equivalent age.

IL-8 is a member of the CXC chemokine family and a mediator of the systemic inflammatory response, where its key role is neutrophil chemotaxis. IL-8 can be secreted by innate and adaptive immune cells and a variety of CNS cells including astrocytes and microglia (Choi et al., 2014; Rustenhoven et al., 2016). IL-8 binds to target cells via the G-protein coupled receptors CXCR1 and CXCR2. These receptors are expressed throughout the CNS and are associated with key

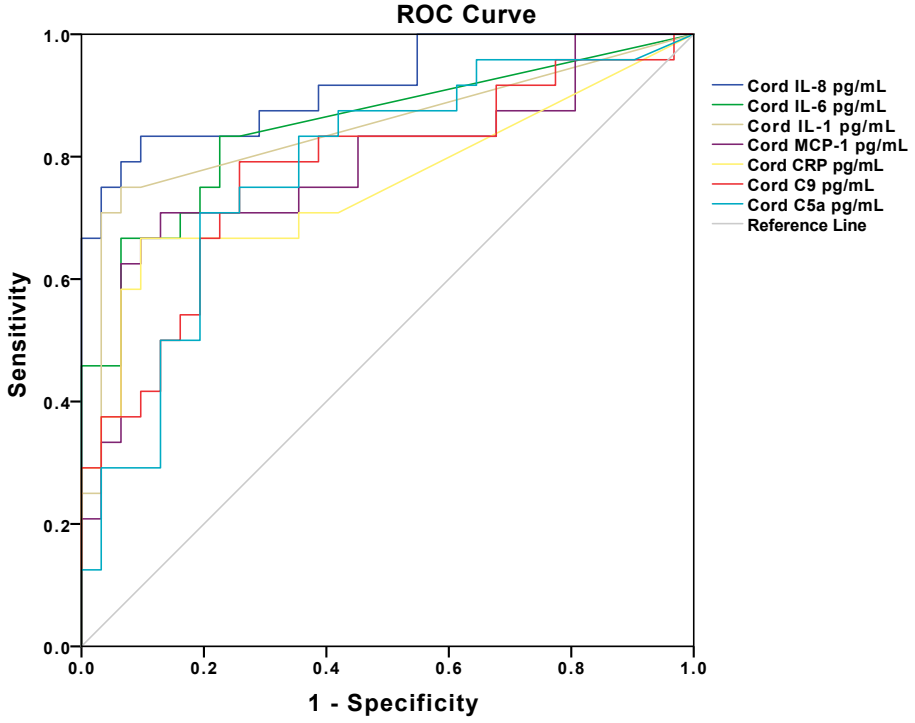

Fig. 2. ROC curve analysis of cord blood inflammatory markers for the prediction of histologic chorioamnionitis.

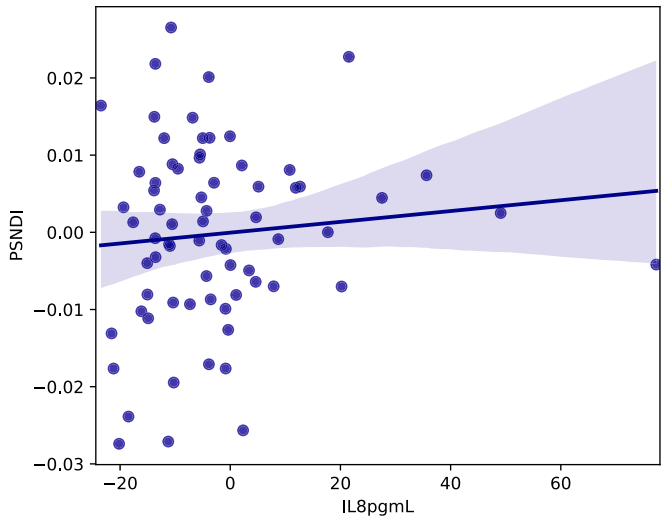

Fig. 3. Partial regression plot of day 5 IL-8 and PSNDI, controlling for GA at birth and GA at scan.

neurodevelopmental processes including cell migration, proliferation and differentiation, oligodendrocyte maturation, axonal growth and synaptic plasticity (Deverman and Patterson, 2009; Semple et al., 2010; Ubogu et al., 2006; Watson et al., 2020). This suggests multiple potential mechanisms through which IL-8 dysregulation during a critical window of neurodevelopment may disrupt healthy CNS development.

IL-8 dysregulation has been implicated in the pathology of several types of human brain injury across the life course. It is associated with blood brain barrier dysfunction in adult traumatic brain injury (Kossmann et al., 1997; Obermeier et al., 2013), with altered cerebral metabolism and poor neurodevelopmental outcome following neonatal hypoxic ischemic injury (Bartha et al., 2004; Foster-Barber et al., 2001) and with increased mortality in children following traumatic brain injury (Woodcock and Morganti-Kossmann, 2013). Studies focused on the perinatal period report that elevated IL-8 in blood sampled from the umbilical cord or soon after birth is associated with overt white matter injury and cerebral palsy, neurodevelopmental impairment, and cognitive impairment in children born preterm, and it is one of the neonatal cytokines that is most strongly associated with subsequent diagnosis of autism among children born at term (Carlo et al., 2011; Hansen-Pupp et al., 2008; Heuer et al., 2019; Kinjo et al., 2011; Kuban et al., 2017, 2014; Leviton et al., 2019; Silveira and Procianoy, 2011). Furthermore, studies investigating the maternal immune activation hypothesis and offspring mental health report that elevated maternal IL-8 during pregnancy is associated with alterations in brain structure and an increased risk of schizophrenia in offspring (Brown et al., 2004; Ellman et al., 2010). This accumulating evidence suggests that inflammation associated with elevated IL-8 has a significant adverse impact on the developing brain with pervasive effects on both structure and function.

To our knowledge, this is the first study to integrate information about systemic inflammation from placenta and blood with biomarkers of white matter microstructure in a representative group of preterm infants without major parenchymal brain injury. We selected a large number of inflammation-associated proteins that are important in the innate and adaptive immune response in the newborn, and used a data driven approach based on PCA to characterize the inflammatory profile associated with HCA and white matter microstructure. Our choice of image features was principled, based on established characterizations of white matter dysmaturation in preterm infants, namely water content and dendritic/axonal complexity and dysmaturation within the white matter skeleton (Blesa et al., 2020; Kunz et al., 2014; Lynch et al., 2020).

A limitation of the study is that the cytokine response is governed not only by environmental insults but also by genetic factors and maternal inflammatory status (Dammann and O'Shea, 2008; Holst and Garnier, 2008; Sheikh et al., 2016). The sample size was not sufficient to perform sub-group analyses based on gestational age or examine potential risks or resilience conferred by the genome, and we did not have data to permit analysis of maternal cytokines. Instead, we characterized antenatal inflammation using placental tissue, which is most closely associated with fetal inflammatory responses (Gotsch et al., 2007). We chose to use a global measure of white matter microstructure because microstructural properties are substantially shared across the major white matter tracts of the newborn brain (Telford et al., 2017), and we hypothesised that systemic inflammation would likely exert a global effect; different methods would be required to investigate hypotheses about tract specific or regional susceptibilities to immune dysregulation.

5. Conclusions

This study provides further support for a substantial role of generalized inflammation in the etiology of preterm brain injury, and it suggests that IL-8 dysregulation may provide a link between systemic inflammation and brain dysmaturation. Further work to assess causation is warranted, such as elucidating cell-specific effects of IL-8 on developing neurons and glia in model systems. Given the potential role of immunomodulatory therapies for treating diseases of the central nervous system (Çakici et al., 2019; Wittenberg et al., 2020), and the availability of anti-IL-8 monoclonal antibody therapies, this finding has implications for the development of perinatal neuroprotection strategies based on anti-inflammatory and novel immune therapeutics.

Declaration of Competing Interest

The authors declare that they have no known competing financial interests or personal relationships that could have appeared to influence the work reported in this paper.

Acknowledgements

We are grateful to the families who consented to participate in the study and to the radiography staff at the Edinburgh Imaging Facility, University of Edinburgh, who participated in infant scanning. This work was supported by Theirworld (www.theirworld.org) and was completed in the MRC Centre for Reproductive Health, at the University of Edinburgh, which is funded by MRC Centre grant (MRC G1002033). M.J.T. was supported by the NHS Lothian Research and Development Office.

Contributions statement

G.S. conceived and designed the study, acquired and analysed data, and drafted the article.

P.G.,M.B.C., M.J.E., M.E.B, A.J.Q. analysed data and revised the article critically for important intellectual content.

N.B-L., K.S. acquired data, analysed data and revised the article critically for important intellectual content.

D.Q.S., M.J.T., G.J.L. acquired data, and revised the article critically for important intellectual content.

S.C. assisted with study design and revised the article critically for important intellectual content.

J.P.B. conceived and designed the study, supervised acquisition of data, analysed data and drafted the article.

All authors approved the final submitted version.

Appendix A. Supplementary data

Supplementary data to this article can be found online at https://doi.org/10.1016/j.bbi.2020.09.007.

References

Anblagan, D., Pataky, R., Evans, M.J., Telford, E.J., Serag, A., Sparrow, S., Piyasena, C., Semple, S.I., Wilkinson, A.G., Bastin, M.E., Boardman, J.P., 2016. Association between preterm brain injury and exposure to chorioamnionitis during fetal life. Sci. Rep. 6 (1). https://doi.org/10.1038/srep37932.

Andersson, J.L.R., Skare, S., Ashburner, J., 2003. How to correct susceptibility distortions in spin-echo echo-planar images: application to diffusion tensor imaging. NeuroImage 20 (2), 870–888.

Andersson, J.L.R., Graham, M.S., Drobnjak, I., Zhang, H., Filippini, N., Bastiani, M., 2017. Towards a comprehensive framework for movement and distortion correction of diffusion MR images: Within volume movement. NeuroImage 152, 450–466.

Andersson, J.L.R., Graham, M.S., Zsoldos, E., Sotiropoulos, S.N., 2016. Incorporating outlier detection and replacement into a non-parametric framework for movement and distortion correction of diffusion MR images. NeuroImage 141, 556–572.

Andersson, J.L.R., Sotiropoulos, S.N., 2016. An integrated approach to correction for off-resonance effects and subject movement in diffusion MR imaging. NeuroImage 125, 1063–1078.

Ball, G., Aljabar, P., Nongena, P., Kennea, N., Gonzalez-Cinca, N., Falconer, S., Chew, A.T.M., Harper, N., Wurie, J., Rutherford, M.A., Counsell, S.J., Edwards, A.D., 2017. Multimodal image analysis of clinical influences on preterm brain development: Clinical Factors and Preterm Brain Development. Ann. Neurol. 82 (2), 233–246.

Barnett, M.L., Tusor, N., Ball, G., Chew, A., Falconer, S., Aljabar, P., Kimpton, J.A., Kennea, N., Rutherford, M., David Edwards, A., Counsell, S.J., 2018. Exploring the multiple-hit hypothesis of preterm white matter damage using diffusion MRI. NeuroImage: Clin. 17, 596–606.

Bartha, A.I., Foster-Barber, A., Miller, S.P., Vigneron, D.B., Glidden, D.V., Barkovich, A.J., Ferriero, D.M., 2004. Neonatal encephalopathy: association of cytokines with MR spectroscopy and outcome. Pediatr. Res. 56 (6), 960–966.

Batalle, D., Hughes, E.J., Zhang, H., Tournier, J.-D., Tusor, N., Aljabar, P., Wali, L., Alexander, D.C., Hajnal, J.V., Nosarti, C., Edwards, A.D., Counsell, S.J., 2017. Early development of structural networks and the impact of prematurity on brain connectivity. NeuroImage 149, 379–392.

Baykara, E., Gesierich, B., Adam, R., Tuladhar, A.M., Biesbroek, J.M., Koek, H.L., Ropele, S., Jouvent, E., Chabriat, H., Ertl-Wagner, B., Ewers, M., Schmidt, R., de Leeuw, F.-E., Biessels, G.J., Dichgans, M., Duering, M., 2016. A novel imaging marker for small vessel disease based on skeletonization of white matter tracts and diffusion histograms: novel SVD imaging marker. Ann. Neurol. 80 (4), 581–592.

Blesa, M., Galdi, P., Sullivan, G., Wheater, E.N., Stoye, D.Q., Lamb, G.J., Quigley, A.J., Thrippleton, M.J., Bastin, M.E., Boardman, J.P., 2020. Peak Width of Skeletonized Water Diffusion MRI in the Neonatal Brain. Front. Neurol. 11.

Boardman, J.P., Craven, C., Valappil, S., Counsell, S.J., Dyet, L.E., Rueckert, D., Aljabar, P., Rutherford, M.A., Chew, A.T.M., Allsop, J.M., Cowan, F., Edwards, A.D., 2010. A common neonatal image phenotype predicts adverse neurodevelopmental outcome in children born preterm. NeuroImage 52, 409–414.

Boardman, J.P., Hall, J., Thrippleton, M.J., Reynolds, R.M., Bogaert, D., Davidson, D.J., Schwarze, J., Drake, A.J., Chandran, S., Bastin, M.E., Fletcher-Watson, S., 2020. Impact of preterm birth on brain development and long-term outcome: protocol for a cohort study in Scotland. BMJ Open 10 (3), e035854.

Boardman, J.P., Ireland, G., Sullivan, G., Pataky, R., Fleiss, B., Gressens, P., Miron, V., 2018. The cerebrospinal fluid inflammatory response to preterm birth. Front. Physiol. 9, 1299.

Brown, A.S., Hooton, J., Schaefer, C.A., Zhang, H., Petkova, E., Babulas, V., Perrin, M., Gorman, J.M., Susser, E.S., 2004. Elevated maternal interleukin-8 levels and risk of schizophrenia in adult offspring. Am. J Psychiatry 161 (5), 889–895.

Çakici, N., van Beveren, N.J.M., Judge-Hundal, G., Koola, M.M., Sommer, I.E.C., 2019. An update on the efficacy of anti-inflammatory agents for patients with schizophrenia: a meta-analysis. Psychol. Med. 49 (14), 2307–2319.

Carlo, W.A., McDonald, S.A., Tyson, J.E., Stoll, B.J., Ehrenkranz, R.A., Shankaran, S., Goldberg, R.N., Das, A., Schendel, D., Thorsen, P., Skogstrand, K., Hougaard, D.M., Oh, W., Laptook, A.R., Duara, S., Fanaroff, A.A., Donovan, E.F., Korones, S.B., Stevenson, D.K., Papile, L.-A., Finer, N.N., O'Shea, T.M., Poindexter, B.B., Wright, L.L., Ambalavanan, N., Higgins, R.D., 2011. Cytokines and neurodevelopmental outcomes in extremely low birth weight infants. J. Pediatrics 159 (6) 919-925.e913.

Chawanpaiboon, S., Vogel, J.P., Moller, A.-B., Lumbiganon, P., Petzold, M., Hogan, D., Landoulsi, S., Jampathong, N., Kongwattanakul, K., Laopaiboon, M., Lewis, C., Rattanakanokchai, S., Teng, D.N., Thinkhamrop, J., Watananirun, K., Zhang, J., Zhou, W., Gülmezoglu, A.M., 2019. Global, regional, and national estimates of levels of preterm birth in 2014: a systematic review and modelling analysis. Lancet Global Health 7 (1), e37–e46.

Choi, S.S., Lee, H.J., Lim, I., Satoh, J., Kim, S.U., 2014. Human astrocytes: secretome profiles of cytokines and chemokines. PloS one 9, e92325.

Dammann, O., O'Shea, T.M., 2008. Cytokines and perinatal brain damage. Clin. Perinatol. 35 (4), 643–663.

Deary, I.J., Ritchie, S.J., Muñoz Maniega, S., Cox, S.R., Valdés Hernández, M.C., Luciano, M., Starr, J.M., Wardlaw, J.M., Bastin, M.E., 2019. Brain Peak Width of Skeletonized Mean Diffusivity (PSMD) and Cognitive Function in Later Life. Frontiers in psychiatry 10, 524.

Deverman, B.E., Patterson, P.H., 2009. Cytokines and CNS Development. Neuron 64 (1), 61–78.

Duggan, P.J., Maalouf, E.F., Watts, T.L., Sullivan, M.H., Counsell, S.J., Allsop, J., Al-Nakib, L., Rutherford, M.A., Battin, M., Roberts, I., Edwards, A.D., 2001. Intrauterine T-cell activation and increased proinflammatory cytokine concentrations in preterm infants with cerebral lesions. The Lancet 358 (9294), 1699–1700.

Ellman, L.M., Deicken, R.F., Vinogradov, S., Kremen, W.S., Poole, J.H., Kern, D.M., Tsai, W.Y., Schaefer, C.A., Brown, A.S., 2010. Structural brain alterations in schizophrenia following fetal exposure to the inflammatory cytokine interleukin-8. Schizophr. Res. 121 (1-3), 46–54.

Foster-Barber, A., Dickens, B., Ferriero, D.M., 2001. Human perinatal asphyxia: correlation of neonatal cytokines with MRI and outcome. Developmental neuroscience 23, 213-218.

Galdi, P., Blesa, M., Stoye, D.Q., Sullivan, G., Lamb, G.J., Quigley, A.J., Thrippleton, M.J., Bastin, M.E., Boardman, J.P., 2020. Neonatal morphometric similarity mapping for predicting brain age and characterizing neuroanatomic variation associated with preterm birth. NeuroImage: Clinical 25, 102195.

Gotsch, F., Romero, R., Kusanovic, J.P., Mazaki-Tovi, S., Pineles, B.L., Erez, O., Espinoza, J., Hassan, S.S., 2007. The fetal inflammatory response syndrome. Clin. Obstetrics Gynecol. 50, 652-683.

Hagberg, H., Mallard, C., Ferriero, D.M., Vannucci, S.J., Levison, S.W., Vexler, Z.S., Gressens, P., 2015. The role of inflammation in perinatal brain injury. Nat. Rev. Neurol. 11 (4), 192–208.

Hansen-Pupp, I., Hallin, A.-L., Hellström-Westas, L., Cilio, C., Berg, A.-C., Stjernqvist, K., Fellman, V., Ley, D., 2008. Inflammation at birth is associated with subnormal development in very preterm infants. Pediatr. Res. 64 (2), 183–188.

Hernandez-Fernandez, M., Reguly, I., Jbabdi, S., Giles, M., Smith, S., Sotiropoulos, S.N., 2019. Using GPUs to accelerate computational diffusion MRI: From microstructure estimation to tractography and connectomes. NeuroImage 188, 598–615.

Heuer, L.S., Croen, L.A., Jones, K.L., Yoshida, C.K., Hansen, R.L., Yolken, R., Zerbo, O., DeLorenze, G., Kharrazi, M., Ashwood, P., Van de Water, J., 2019. An exploratory examination of neonatal cytokines and chemokines as predictors of autism risk: the early markers for autism study. Biol. Psychiatry 86 (4), 255–264.

Holst, D., Garnier, Y., 2008. Preterm birth and inflammation—the role of genetic polymorphisms. Eur. J. Obstetrics Gynecol. Reproductive Biol. 141 (1), 3–9.

Jenkinson, M., Beckmann, C.F., Behrens, T.E.J., Woolrich, M.W., Smith, S.M., 2012. FSL. NeuroImage 62 (2), 782–790.

Kapellou, O., Counsell, S.J., Kennea, N., Dyet, L., Saeed, N., Stark, J., Maalouf, E., Duggan, P., Ajayi-Obe, M., Hajnal, J., Allsop, J.M., Boardman, J., Rutherford, M.A., Cowan, F., Edwards, A.D., 2006. Abnormal cortical development after premature birth shown by altered allometric scaling of brain growth. PLoS Med. 3, e265.

Kinjo, T., Ohga, S., Ochiai, M., Honjo, S., Tanaka, T., Takahata, Y., Ihara, K., Hara, T., 2011. Serum chemokine levels and developmental outcome in preterm infants. Early Human Dev. 87 (6), 439–443.

Kossmann, T., Stahel, P.F., Lenzlinger, P.M., Redl, H., Dubs, R.W., Trentz, O., Schlag, G., Morganti-Kossmann, M.C., 1997. Interleukin-8 released into the cerebrospinal fluid after brain injury is associated with blood–brain barrier dysfunction and nerve growth factor production. J. Cereb. Blood Flow Metab. 17 (3), 280–289.

Kuban, K.C., Joseph, R.M., O'Shea, T.M., Heeren, T., Fichorova, R.N., Douglass, L., Jara, H., Frazier, J.A., Hirtz, D., Rollins, J.V., Paneth, N., 2017. Circulating inflammatory-associated proteins in the first month of life and cognitive impairment at age 10 years in children born extremely preterm. J. Pediatrics 180, 116-123.e111.

Kuban, K.C.K., O'Shea, T.M., Allred, E.N., Paneth, N., Hirtz, D., Fichorova, R.N., Leviton, A., 2014. Systemic Inflammation and Cerebral Palsy Risk in Extremely Preterm Infants. J. Child Neurol. 29 (12), 1692–1698.

Kunz, N., Zhang, H., Vasung, L., O'Brien, K.R., Assaf, Y., Lazeyras, F., Alexander, D.C., Hüppi, P.S., 2014. Assessing white matter microstructure of the newborn with multi-shell diffusion MRI and biophysical compartment models. NeuroImage 96, 288–299.

Leuchter, R.-V., Gui, L., Poncet, A., Hagmann, C., Lodygensky, G.A., Martin, E., Koller, B., Darqué, A., Bucher, H.U., Hüppi, P.S., 2014. Association between early administration of high-dose erythropoietin in preterm infants and brain MRI abnormality at term-equivalent age. JAMA 312 (8), 817.

Leviton, A., Allred, E.N., Fichorova, R.N., Kuban, K.C.K., Michael O'Shea, T., Dammann, O., 2016. Systemic inflammation on postnatal days 21 and 28 and indicators of brain dysfunction 2years later among children born before the 28th week of gestation. Early Human Dev. 93, 25–32.

Leviton, A., Allred, E.N., Fichorova, R.N., O'Shea, T.M., Fordham, L.A., Kuban, K.K.C., Dammann, O., 2018. Circulating biomarkers in extremely preterm infants associated with ultrasound indicators of brain damage. Eur. J. Paediatric Neurol. 22 (3), 440–450.

Leviton, A., Joseph, R.M., Fichorova, R.N., Allred, E.N., Gerry Taylor, H., Michael O'Shea, T., Dammann, O., 2019. Executive dysfunction early postnatal biomarkers among children born extremely preterm. J. Neuroimmune Pharmacol. 14 (2), 188–199.

Lynch, K.M., Cabeen, R.P., Toga, A.W., Clark, K.A., 2020. Magnitude and timing of major white matter tract maturation from infancy through adolescence with NODDI. NeuroImage 212, 116672.

O'Shea, T.M., Allred, E.N., Kuban, K.C.K., Dammann, O., Paneth, N., Fichorova, R., Hirtz, D., Leviton, A., 2012. Elevated concentrations of inflammation-related proteins in postnatal blood predict severe developmental delay at 2 years of age in extremely preterm infants. J. Pediatrics 160 (3) 395-401.e394.

O'Shea, T.M., Shah, B., Allred, E.N., Fichorova, R.N., Kuban, K.C.K., Dammann, O., Leviton, A., 2013. Inflammation-initiating illnesses, inflammation-related proteins, and cognitive impairment in extremely preterm infants. Brain Behav. Immun. 29, 104–112.

Obermeier, B., Daneman, R., Ransohoff, R.M., 2013. Development, maintenance and disruption of the blood-brain barrier. Nat. Med. 19 (12), 1584–1596.

Pecheva, D., Kelly, C., Kimpton, J., Bonthrone, A., Batalle, D., Zhang, H., Counsell, S.J.,

2018. Recent advances in diffusion neuroimaging: applications in the developing preterm brain. F1000Res 7, 1326.
Pietsch, M., Christiaens, D., Hutter, J., Cordero-Grande, L., Price, A.N., Hughes, E., Edwards, A.D., Hajnal, J.V., Counsell, S.J., Tournier, J.-D., 2019. A framework for multi-component analysis of diffusion MRI data over the neonatal period. NeuroImage 186, 321–337.
Redline, R.W., Faye-Petersen, O., Heller, D., Qureshi, F., Savell, V., Vogler, C., 2003. Amniotic infection syndrome: nosology and reproducibility of placental reaction patterns. Pediatr. Dev. Pathol. 6 (5), 435–448.
Rustenhoven, J., Park, T.-H., Schweder, P., Scotter, J., Correia, J., Smith, A.M., Gibbons, H.M., Oldfield, R.L., Bergin, P.S., Mee, E.W., Faull, R.L.M., Curtis, M.A., Scott Graham, E., Dragunow, M., 2016. Isolation of highly enriched primary human microglia for functional studies. Sci. Rep. 6 (1).
Semple, B.D., Kossmann, T., Morganti-Kossmann, M.C., 2010. Role of chemokines in CNS health and pathology: a focus on the CCL2/CCR2 and CXCL8/CXCR2 networks. J. Cereb. Blood Flow Metab. 30 (3), 459–473.
Shah, D.K., Doyle, L.W., Anderson, P.J., Bear, M., Daley, A.J., Hunt, R.W., Inder, T.E., 2008. Adverse neurodevelopment in preterm infants with postnatal sepsis or necrotizing enterocolitis is mediated by white matter abnormalities on magnetic resonance imaging at term. J. Pediatrics 153 (2) 175.e171.
Sheikh, I.A., Ahmad, E., Jamal, M.S., Rehan, M., Assidi, M., Tayubi, I.A., AlBasri, S.F., Bajouh, O.S., Turki, R.F., Abuzenadah, A.M., Damanhouri, G.A., Beg, M.A., Al-Qahtani, M., 2016. Spontaneous preterm birth and single nucleotide gene polymorphisms: a recent update. BMC Genomics 17 (S9).
Silveira, R.C., Procianoy, R.S., 2011. High plasma cytokine levels, white matter injury and neurodevelopment of high risk preterm infants: Assessment at two years. Early Human Dev. 87 (6), 433–437.
Skogstrand, K., Hougaard, D.M., Schendel, D.E., Bent, N.P., Svaerke, C., Thorsen, P., 2008. Association of preterm birth with sustained postnatal inflammatory response. Obstetrics and gynecology 111, 1118-1128.
Tariq, M., Schneider, T., Alexander, D.C., Gandini Wheeler-Kingshott, C.A., Zhang, H., 2016. Bingham–NODDI: mapping anisotropic orientation dispersion of neurites using diffusion MRI. NeuroImage 133, 207–223.
Telford, E.J., Cox, S.R., Fletcher-Watson, S., Anblagan, D., Sparrow, S., Pataky, R., Quigley, A., Semple, S.I., Bastin, M.E., Boardman, J.P., 2017. A latent measure explains substantial variance in white matter microstructure across the newborn human brain. Brain Struct. Funct. 222 (9), 4023–4033.
Tournier, J.-D., Smith, R., Raffelt, D., Tabbara, R., Dhollander, T., Pietsch, M., Christiaens, D., Jeurissen, B., Yeh, C.-H., Connelly, A., 2019. MRtrix3: a fast, flexible and open software framework for medical image processing and visualisation. NeuroImage 202, 116137.
Tustison, N.J., Avants, B.B., Cook, P.A., Zheng, Y., Egan, A., Yushkevich, P.A., Gee, J.C., 2010. N4ITK: improved N3 bias correction. IEEE Trans. Med. Imaging 29 (6), 1310–1320.
Twilhaar, E.S., Wade, R.M., de Kieviet, J.F., van Goudoever, J.B., van Elburg, R.M., Oosterlaan, J., 2018. Cognitive outcomes of children born extremely or very preterm since the 1990s and associated risk factors: a meta-analysis and meta-regression. JAMA Pediatr 172 (4), 361.
Ubogu, E.E., Cossoy, M.B., Ransohoff, R.M., 2006. The expression and function of chemokines involved in CNS inflammation. Trends Pharmacol. Sci. 27 (1), 48–55.
Veraart, J., Novikov, D.S., Christiaens, D., Ades-aron, B., Sijbers, J., Fieremans, E., 2016. Denoising of diffusion MRI using random matrix theory. NeuroImage 142, 394–406.
Volpe, J.J., 2019. Dysmaturation of premature brain: importance, cellular mechanisms, and potential interventions. Pediatr. Neurol. 95, 42–66.
Watson, A.E.S., Goodkey, K., Footz, T., Voronova, A., 2020. Regulation of CNS precursor function by neuronal chemokines. Neurosci. Lett. 715, 134533.
Wei, N., Deng, Y., Yao, L., Jia, W., Wang, J., Shi, Q., Chen, H., Pan, Y., Yan, H., Zhang, Y., Wang, Y., 2019. A Neuroimaging Marker Based on Diffusion Tensor Imaging and Cognitive Impairment Due to Cerebral White Matter Lesions. Frontiers in neurology 10.
Wittenberg, G.M., Stylianou, A., Zhang, Y., Sun, Y.u., Gupta, A., Jagannatha, P.S., Wang, D., Hsu, B., Curran, M.E., Khan, S., Chen, G., Bullmore, E.T., Drevets, W.C., 2020. Effects of immunomodulatory drugs on depressive symptoms: a mega-analysis of randomized, placebo-controlled clinical trials in inflammatory disorders. Mol. Psychiatry 25 (6), 1275–1285.
Woodcock, T., Morganti-Kossmann, M.C., 2013. The role of markers of inflammation in traumatic brain injury. Front. Neurol. 4, 18.
Yanni, D., Korzeniewski, S.J., Allred, E.N., Fichorova, R.N., O'Shea, T.M., Kuban, K., Dammann, O., Leviton, A., 2017. Both antenatal and postnatal inflammation contribute information about the risk of brain damage in extremely preterm newborns. Pediatr. Res. 82 (4), 691–696.
Yoon, B.H., Romero, R., Yang, S.H., Jun, J.K., Kim, I.-O., Choi, J.-H., Syn, H.C., 1996. Interleukin-6 concentrations in umbilical cord plasma are elevated in neonates with white matter lesions associated with periventricular leukomalacia. Am. J. Obstet. Gynecol. 174 (5), 1433–1440.
Zhang, H., Schneider, T., Wheeler-Kingshott, C.A., Alexander, D.C., 2012. NODDI: Practical in vivo neurite orientation dispersion and density imaging of the human brain. NeuroImage 61 (4), 1000–1016.
Zhang, H., Yushkevich, P., Alexander, D., Gee, J., 2006. Deformable registration of diffusion tensor MR images with explicit orientation optimization. Med. Image Anal. 10 (5), 764–785.